PHYSICAL REVIEW B **87**, 121303(R) (2013)

Coulomb-driven organization and enhancement of spin-orbit fields in collective spin excitations

F. Baboux,[1,*] F. Perez,[1,†] C. A. Ullrich,[2] I. D'Amico,[3] G. Karczewski,[4] and T. Wojtowicz[4]

[1]*Institut des Nanosciences de Paris, CNRS/Université Paris VI, Paris 75005, France*

[2]*Department of Physics and Astronomy, University of Missouri, Columbia, Missouri 65211, USA*

[3]*Department of Physics, University of York, York YO10 5DD, United Kingdom*

[4]*Institute of Physics, Polish Academy of Sciences, Warsaw, Poland*

(Received 14 December 2012; revised manuscript received 22 January 2013; published 21 March 2013)

Spin-orbit (SO) fields in a spin-polarized electron gas are studied by angle-resolved inelastic light scattering on a CdMnTe quantum well. We demonstrate a striking organization and enhancement of SO fields acting on the collective spin excitation (spin-flip wave). While individual electronic SO fields have a broadly distributed momentum dependence, giving rise to D'yakonov-Perel' dephasing, the collective spin dynamics is governed by a single *collective* SO field which is drastically enhanced due to many-body effects. The enhancement factor is experimentally determined. These results provide a powerful indication that these constructive phenomena are universal to collective spin excitations of conducting systems.

DOI: 10.1103/PhysRevB.87.121303 PACS number(s): 71.70.Ej, 72.25.Rb, 73.21.−b, 78.30.−j

An electron moving with momentum $\mathbf{k}$ in an electric field $\mathbf{E}$ experiences an effective magnetic field $\mathbf{B}_{\mathrm{SO}}(\mathbf{k}) \propto \mathbf{E} \times \mathbf{k}$ that couples to its spin. In semiconductor nanostructures, this spin-orbit (SO) coupling arises through internal electric fields[1] and opens promising ways to manipulate the electronic spin through, e.g., current-induced spin polarization,[2] spin Hall currents,[3] or zero-bias spin separation.[4] However, SO coupling generally causes also losses of spin memory: due to the momentum dependence of SO fields, each individual spin of an ensemble precesses with its own frequency and axis (D'yakonov-Perel' decoherence[5]). In recent years, numerous efforts have been made to overcome this decoherence, by using structure engineering,[6] control by gate electrodes,[7,8] or spin-echo-type techniques.[9,10]

Recently, an alternative promising path was initiated[11] by discovering that a particular collective spin excitation, the intersubband spin-plasmon of a GaAs quantum well, is *intrinsically* protected from D'yakonov-Perel' decoherence. Indeed, Coulomb interaction rearranges the distribution of SO fields, so that all electronic spins precess in synchronicity about a single *collective* SO field.

In addition, this collective SO field was discovered to be drastically enhanced with respect to the one acting on individual electrons. Indeed, for noncollective spin excitations such as a spin packet drifting with momentum $\mathbf{q}$, the relevant SO field is that which would act on a single electron of same momentum, $\mathbf{B}_{\mathrm{SO}}(\mathbf{q})$.[2,7,10,12,13] By contrast, the SO field acting on the intersubband spin-plasmon, $\mathbf{B}_{\mathrm{SO}}^{\mathrm{coll}}(\mathbf{q})$, is very strongly enhanced: it was found in Ref. 11 that $\mathbf{B}_{\mathrm{SO}}^{\mathrm{coll}}(\mathbf{q}) \approx 5\, \mathbf{B}_{\mathrm{SO}}(\mathbf{q})$.

This raises the important question whether these constructive phenomena are bound to the peculiar nature of the intersubband spin-plasmon of a GaAs quantum well, or are fully general to collective spin excitations of any conducting system. Here, we evidence them in another configuration: we study the intrasubband spin-flip wave (SFW) of a spin-polarized electron gas confined in a diluted magnetic semiconductor (DMS).[14–16] Thus we provide a powerful indication of the universality of the immunity against dephasing, and giant enhancement of SO effects at the collective level. In addition, as we shall see, the system studied here allows for a much simpler demonstration of these effects; here, in contrast to Ref. 11, direct observations of the SO fields at *both* the single-particle and the collective level can be made. This allows for a fully experimental determination of the SO enhancement factor, and shows that DMS quantum wells are ideal systems for future study and functionalization of collective SO effects.

We carry out inelastic light scattering (ILS) measurements on an asymmetrically modulation-doped, 30-nm-thick $Cd_{1-x}Mn_xTe$ quantum well of high mobility, grown along the [001] direction by molecular beam epitaxy. The electronic density is $n_{2D} = 3.5 \times 10^{11}$ cm^{-2} and the mobility 10^5 cm^2/Vs, as determined from magnetotransport measurements. ILS is a powerful tool to transfer a momentum $\mathbf{q}$ to the spin excitations of the two-dimensional electron gas (2DEG).[14,17] In our setup, depicted in Fig. 1(a), $\mathbf{q}$ can be varied both in amplitude and in-plane orientation. A magnetic field $\mathbf{B}_{\mathrm{ext}}$ is applied in the plane of the well, always perpendicular to $\mathbf{q}$. φ denotes the angle between $\mathbf{q}$ and the [100] crystallographic direction of the well. The incoming and scattered light polarizations are crossed, which is the required selection rule to address spin-flip excitations.[14,17]

Figure 1(b) shows a typical ILS spectrum obtained for $q \simeq 0$, at superfluid helium bath temperature ($T \sim 2$ K). Here $B_{\mathrm{ext}} = 3$ T and $\varphi = \pi/4$. The spectrum shows two kinds of excitations:[14,15] a narrow peak corresponding to the SFW (energy Z) and, at higher energy, a broader line corresponding to spin-flip single-particle excitations[18] (SPE, of center energy Z^*). The energy of both excitations is plotted as a function of B_{ext} in Fig. 1(c). The $q = 0$ SFW involves a parallel precession of all electron spins. Thus, its energy does not depend on Coulomb interaction, owing to Larmor's theorem,[14] and follows the giant Zeeman splitting of conduction electrons:[19]

$$Z(B_{\mathrm{ext}}) = -\overline{x} J_{s-d} \langle S_z(B_{\mathrm{ext}}) \rangle_{\mathrm{th}} + g \mu_{\mathrm{B}} B_{\mathrm{ext}}. \qquad (1)$$

This is the sum of two opposite contributions (one due to the exchange field created by the polarized Mn, and one directly due to B_{ext}), explaining the non-monotonic variation of Z with B_{ext}. $J_{s-d} = 0.22$ eV is the exchange integral[19] for conduction electrons in $Cd_{1-x}Mn_xTe$, $\overline{x}$ the effective Mn concentration ($\overline{x} \simeq x$ for low x), $\langle S_z(B_{\mathrm{ext}}) \rangle_{\mathrm{th}}$ is the thermally averaged spin of a single Mn^{2+} ion (negative for $B_{\mathrm{ext}} > 0$), μ_{B} the Bohr magneton and $g = -1.64$ the electronic g factor.

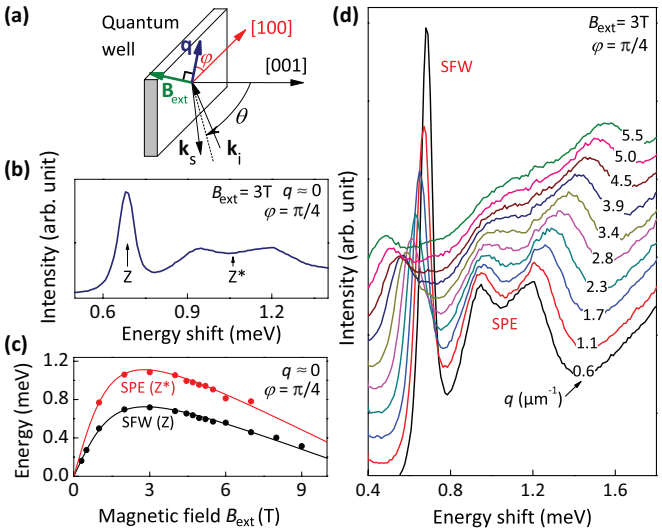

FIG. 1. (Color online) Intrasubband spin excitations of a CdMnTe quantum well. (a) Scattering geometry: $\mathbf{k_i}$ and $\mathbf{k_s}$ are the incoming and scattered light wave vectors; $\mathbf{q}$ is the transferred momentum, of in-plane orientation φ measured from [100], and amplitude $|\mathbf{q}| \simeq \frac{4\pi}{\lambda}\sin\theta$, where $\lambda \simeq 771$ nm is the incoming wavelength. An external magnetic field $\mathbf{B}_{ext}$ is applied perpendicularly to $\mathbf{q}$ (the arrow defines $B_{ext} > 0$). (b) Typical inelastic light scattering (ILS) spectrum obtained at $q \simeq 0$ in cross-polarized geometry. Two lines are observed, corresponding to the spin-flip wave (SFW, energy Z) and to the spin-flip single-particle excitations (SPE, energy Z^*). (c) Magnetic dispersion of Z and Z^*. (d) ILS spectra obtained for $B_{ext} = 3$ T and a series of transferred momenta q, at fixed in-plane angle $\varphi = \pi/4$.

A fit of the SFW energy to Eq. (1) yields $x = 0.215\,\%$ and $T = 2.6$ K. In contrast to the SFW, flipping the spin of a single electron without disturbance of other spins costs an additional Coulomb-exchange energy due to Pauli repulsion: the center of the SPE line thus lies at a higher energy,[15] the Coulomb-renormalized Zeeman energy Z^*.

We now turn to the wave-vector dispersion of both excitations. In Fig. 1(d), we plot spectra obtained at fixed $B_{ext} = 3$ T and $\varphi = \pi/4$, but various magnitudes of the transferred momentum $\mathbf{q}$. The energy of the SFW decreases with increasing q. Indeed, spins in a $q \neq 0$ SFW mode are periodically antiparallel for each π/q: compared to the $q = 0$ situation, this induces a reduction in the Coulomb-exchange repulsion more and more pronounced as π/q is lowered, yielding a downward dispersion. The interplay between Coulomb interaction and the kinetic energy leads to a parabolic dispersion for the SFW energy (to leading order in q):[20]

$$E(q) = \left| Z - \frac{1}{\zeta}\frac{Z}{Z^* - Z}\frac{\hbar^2}{2m_b}q^2 \right| \equiv |Z - fq^2|, \qquad (2)$$

where $\zeta = (m_b/2\pi\hbar^2 n_{2D})Z^*$ is the spin polarization and m_b is the band mass.

However, this expression ignores anisotropic effects stemming from SO coupling. To investigate such effects, we plot in Fig. 2 the SFW energy as a function of the in-plane angle φ, for $B_{ext} = 3$ T (a) and $B_{ext} = -3$ T (b), and for three values of the momentum q. Several salient features are observed: (i) the SFW energy shows a sine-type modulation

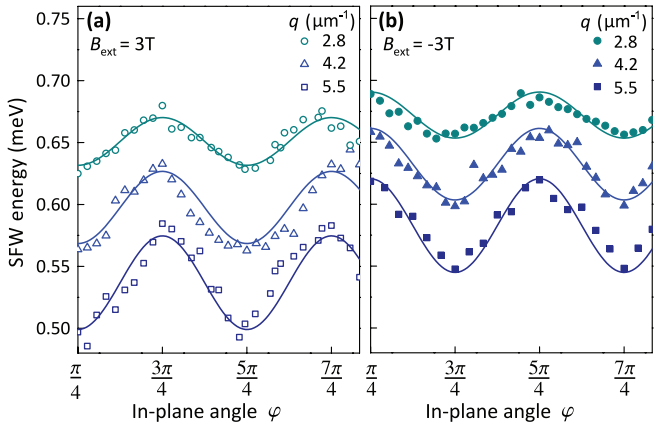

FIG. 2. (Color online) Spin-orbit induced modulation of the spin-flip wave energy, (a) for $B_{ext} = 3$ T and (b) $B_{ext} = -3$ T, and for three amplitudes of the transferred momentum q. The modulation shows a two-fold symmetry, and its amplitude increases with q. Furthermore, as compared with $B_{ext} > 0$, the modulation for $B_{ext} < 0$ is out of phase, and lies at higher energy. The lines reproduce Eq. (6).

with a twofold symmetry, analogous to the one found for intersubband spin-plasmons[11] as well as in Ref. 21 for similar CdMnTe quantum wells. In addition, (ii) the amplitude of this modulation increases with growing q; (iii) the modulations obtained for $B_{ext} > 0$ and $B_{ext} < 0$ are out of phase, and (iv) the latter lies on average at higher energy than the former.

To understand these features, let us consider the total Hamiltonian of the system, containing kinetic, Coulomb, Zeeman, and SO contributions: $\widehat{\mathcal{H}}_{tot} = \widehat{\mathcal{H}}_{Kin} + \widehat{\mathcal{H}}_{Coul} + \widehat{\mathcal{H}}_{Z} + \widehat{\mathcal{H}}_{SO}$. The SO part reads $\widehat{\mathcal{H}}_{SO} = \sum \mathbf{B}_{SO}(\mathbf{k}) \cdot \widehat{\boldsymbol{\sigma}}/2$, where the sum runs over all electrons of momentum $\mathbf{k}$ and spin $\widehat{\boldsymbol{\sigma}}$ (Pauli operators). $\mathbf{B}_{SO}(\mathbf{k})$ is an in-plane field, whose magnitude determines the SO-induced spin splitting at momentum $\mathbf{k}$. It arises from the asymmetry of the confining potential (Rashba effect[22]) and that of the crystalline cell (Dresselhaus effect[23]):

$$\mathbf{B}_{SO}(\mathbf{k}) = 2\alpha\,(k_y, -k_x) + 2\beta\,(k_x, -k_y) \qquad (3)$$

with $\hat{x} \parallel [100]$ and $\hat{y} \parallel [010]$, and with α and β the Rashba and linear Dresselhaus coupling constants,[1] respectively.

The excitations of $\widehat{\mathcal{H}}_{tot}$, including the SFW, can in principle be calculated in linear response theory.[24] Instead, we will propose a phenomenological model in line with the one validated in Ref. 11 for the intersubband spin-plasmon. This collective excitation was shown to behave as a macroscopic quantum object of spin magnitude 1, subject to a collective SO field proportional to the excitation momentum $\mathbf{q}$:

$$\mathbf{B}_{SO}^{coll}(\mathbf{q}) = 2\widetilde{\alpha}\,(q_y, -q_x) + 2\widetilde{\beta}\,(q_x, -q_y)\,, \qquad (4)$$

where $\widetilde{\alpha}$ and $\widetilde{\beta}$ are the *collective* Rashba and Dresselhaus coupling constants, respectively.

We will assume that the SFW also behaves as a spin 1 object, immersed in the above collective SO field, as well as the Coulomb-exchange field leading to the dispersion of Eq. (2). Reducing the system to the SFW only, we are left to study the following effective Hamiltonian:

$$\widehat{\mathcal{H}}_{SFW} = \widehat{\mathbf{S}} \cdot \left[|Z - fq^2| \frac{\mathbf{B}_{ext}}{|B_{ext}|} + \mathbf{B}_{SO}^{coll}(\mathbf{q}) \right], \qquad (5)$$

where $\widehat{\boldsymbol{S}}$ is the vector of spin matrices for a spin 1. Only the eigenstate with positive energy, corresponding to a SFW mode with spin projection $+1$, is addressable experimentally.[20] Since the modulation of Fig. 2 does not exceed 10% of Z, we consider this eigenenergy to leading order in $\widetilde{\alpha}q/Z$ and $\widetilde{\beta}q/Z$, yielding the SFW dispersion $E(q,\varphi) = |Z - fq^2 - 2\widetilde{\alpha}q - 2\widetilde{\beta}q \sin 2\varphi|$. This expression reproduces the sinusoidal modulation of the SFW energy with a two-fold symmetry, and its increase in amplitude with q [properties (i) and (ii) above]. We further note that $(Z - fq^2)$ has the same sign as $B_{\rm ext}$; thus, if $E_\pm$ denotes the SFW energy for $B_{\rm ext} \gtrless 0$,

$$E_\pm(q,\varphi) = |Z - fq^2| \mp 2\widetilde{\alpha}q \mp 2\widetilde{\beta}q \sin 2\varphi. \qquad (6)$$

Hence $\widetilde{\beta}$ governs the *amplitude* of the SO modulation, with opposite signs for $B_{\rm ext} > 0$ and $B_{\rm ext} < 0$. This qualitatively explains property (iii) above. As for $\widetilde{\alpha}$, it governs the *energy offset* between the two situations, $B_{\rm ext} > 0$ and $B_{\rm ext} < 0$, explaining property (iv).

In the following, we will consider four specific experimental situations that allow us to extract $\widetilde{\alpha}$ and $\widetilde{\beta}$. These are schematized in Fig. 3(a): for $\varphi = \pi/4$ and $\varphi = 3\pi/4$, the Rashba component of the collective SO field ($\mathbf{B}^{\rm coll}_{\rm SO,R}$), the Dresselhaus component ($\mathbf{B}^{\rm coll}_{\rm SO,D}$), and the external field are collinear, yielding extrema in the SFW energy. Figure 3(b) shows the corresponding experimental dispersions (the same color code is used), obtained at $|B_{\rm ext}| = 3$ T. For $B_{\rm ext} > 0$, the energy difference between $\varphi = \pi/4$ and $\varphi = 3\pi/4$, $E_+(q,3\pi/4) - E_+(q,\pi/4)$, yields $4\widetilde{\beta}q$ according to Eq. (6). Similarly, the same difference for $B_{\rm ext} < 0$ is $-4\widetilde{\beta}q$. We plot the latter quantities in Fig. 3(c) for previous data (circles) as well as for additional data taken at $|B_{\rm ext}| = 2$ and 4 T (squares and triangles). A linear behavior is indeed observed, independent of the external magnetic field within the error, in agreement with Eq. (6). Averaging over all magnetic field values, we find $\widetilde{\beta} = 31.6 \pm 4.5$ meVÅ.

The collective Rashba coefficient $\widetilde{\alpha}$ can be extracted from the energy offset between $B_{\rm ext} > 0$ and $B_{\rm ext} < 0$. Indeed, if $\langle E_\pm \rangle(q) = [E_\pm(q,3\pi/4) + E_\pm(q,\pi/4)]/2$ denotes the angular average of the SFW energy, the difference $\langle E_- \rangle(q) - \langle E_+ \rangle(q)$ equals $4\widetilde{\alpha}q$ according to Eq. (6). This quantity is plotted in Fig. 3(d) for $|B_{\rm ext}| = 2,3$ and 4 T. Again, very good agreement is found with the predicted linearity, independent of the applied magnetic field. We deduce $\widetilde{\alpha} = 19.9 \pm 2.5$ meVÅ.

Finally, Z and the quadratic coefficient f of the dispersion are determined from the mean dispersion $[\langle E_- \rangle(q) + \langle E_+ \rangle(q)]/2$, where all SO terms are averaged out. The consistency of the model defined by Eq. (5) is demonstrated in Figs. 2(a)–2(b) and Fig. 3(b), where we plot the relation of Eq. (6) (lines) using the above extracted parameters; the experimental SFW energy is very well reproduced.

The above determination of $\widetilde{\alpha}$ and $\widetilde{\beta}$ highlights the key advantage of the spin-polarized 2DEG to study collective SO effects. In contrast to the intersubband spin-plasmons studied in Ref. 11, collective SO effects here directly show up as a modulation of the SFW energy [see Eq. (6)]. In addition, as we shall now see, SO effects at the single-particle level can here be experimentally resolved. Figure 4(a) shows spectra obtained at $B_{\rm ext} = 3$ T and $q = 0.6$ μm^{-1}, for a series of equally spaced orientations between $\varphi = \pi/4$ (bottom curve) and $\varphi = 3\pi/4$ (top curve). A strong in-plane modulation of the SPE line occurs, as a result of the interplay between the external magnetic field and the internal SO fields. The latter modulate the Fermi contour of each spin population, with

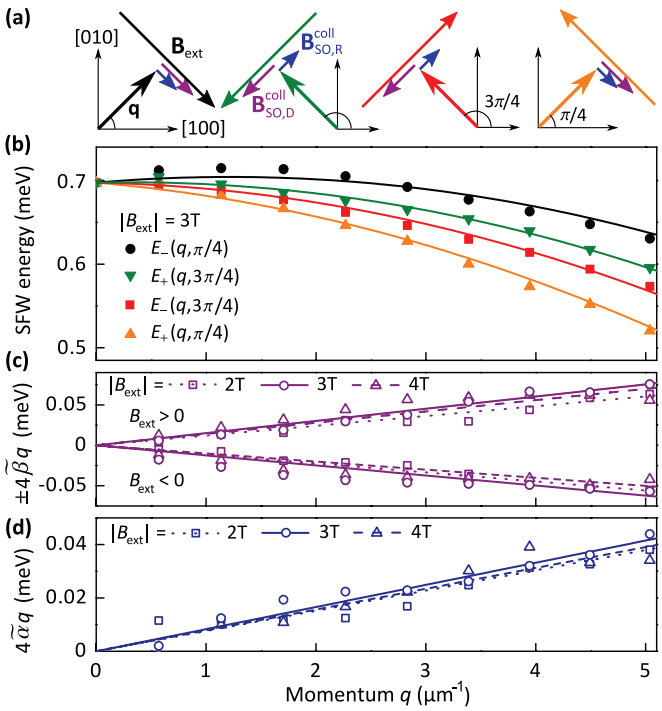

FIG. 3. (Color online) Extraction of the collective spin-orbit coupling constants. (a) Schematics of the four experimental configurations $(\varphi, B_{\rm ext})$ used to extract $\widetilde{\alpha}$ and $\widetilde{\beta}$. $\mathbf{B}^{\rm coll}_{\rm SO,R}$ is the Rashba component of the collective SO field (blue), and $\mathbf{B}^{\rm coll}_{\rm SO,D}$ the Dresselhaus component (purple). (b) SFW dispersions obtained for the configurations depicted above (same color code). Lines correspond to Eq. (6). (c) For $|B_{\rm ext}| = 2$, 3 and 4 T, plots of $E_\pm(q,3\pi/4) - E_\pm(q,\pi/4)$. Both quantities are linear in q. (d) For the same values of $|B_{\rm ext}|$, plots of the quantity $\langle E_- \rangle(q) - \langle E_+ \rangle(q)$.

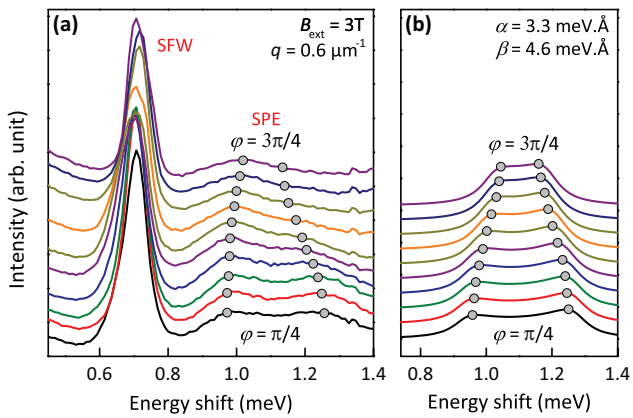

FIG. 4. (Color online) Extraction of the individual spin-orbit coupling constants. (a) Experimental ILS spectra obtained at $B_{\rm ext} = 3$ T and $q = 0.6$ μm^{-1}, for a series of equally spaced in-plane orientations between $\varphi = \pi/4$ (bottom curve) and $\varphi = 3\pi/4$ (top curve). (b) With the same color code, calculated imaginary part of the Lindhard polarizability of Eq. (7) using $\alpha = 3.3$ meVÅ and $\beta = 4.6$ meVÅ. The grey points are guides to the eye.

a twofold in-plane symmetry.[25] Van Hove-type singularities in the joint density of states appear when both contours are locally parallel.[26] This gives rise to the two shoulders observed in the SPE line.[27] The separation between both shoulders reflects the spread of single-particle SO fields due to their momentum dependence, in strong contrast with the SFW, which produces a sharp line. This provides a clear manifestation of the organization of SO fields at the collective level.

To extract α and β [see Eq. (3)], we calculate the spin-flip Lindhard polarizability[28]

$$\Pi_{\downarrow\uparrow}(\mathbf{q},\omega) = \int \frac{d^2\mathbf{k}}{(2\pi)^2} \frac{n(\epsilon_{\mathbf{k}\downarrow}) - n(\epsilon_{\mathbf{k}+\mathbf{q}\uparrow})}{\epsilon_{\mathbf{k}\downarrow} - \epsilon_{\mathbf{k}+\mathbf{q}\uparrow} + \hbar\omega + i\eta}, \qquad (7)$$

whose imaginary part describes the shape of the spin-flip SPE line[26] at transferred momentum $\mathbf{q}$. n denotes the Fermi occupation function, $\epsilon_{\mathbf{k}\sigma}$ is the energy of a single-particle state of momentum $\mathbf{k}$ and spin $\sigma = \uparrow$ or $\downarrow$,[29] and η accounts for the finite lifetime $\hbar/\eta$ of quasielectrons due to scattering off disorder and other electrons. In the approximation of strong external field used above [see Eq. (6)], $\epsilon_{\mathbf{k}\sigma} \simeq \frac{\hbar^2 k^2}{2m_b} + \sigma\,\mathrm{sgn}(B_{\mathrm{ext}})\big(Z^*/2 - \big[\alpha\cos(\varphi-\varphi_{\mathbf{k}}) + \beta\sin(\varphi+\varphi_{\mathbf{k}})\big]k\big)$, where $\mathrm{sgn}(B_{\mathrm{ext}})$ is the sign of B_{ext}, $\sigma = \pm 1$ and $\varphi_{\mathbf{k}}$ is the angle between $\mathbf{k}$ and the [100] direction of the well.

Figure 4(b) shows the calculated imaginary part of $\Pi_{\downarrow\uparrow}$ for the experimental parameters of Fig. 4(a) (same color code). The main experimental trend is well reproduced by using $\alpha = 3.3$ meVÅ, $\beta = 4.6$ meVÅ and $\eta = 0.05$ meV. Note that the fitted disorder parameter η (which affects the softening of the line shape, but not the magnitude of the splitting) is at least three times lower than for previously investigated samples,[15,16,30] confirming a very high sample quality. Indeed, Fig. 4(a) is to our knowledge the first ILS observation of a SO splitting in the SPE line of a DMS quantum well.

The measured α and β can be compared to theoretical estimates. The Rashba coefficient can be calculated from $\alpha = r_{41}^{6c6c} e\langle E_z\rangle$, with e the electronic charge and $\langle E_z\rangle$ the average electric field along the growth axis. Assuming that the electrons experience the delta-doping layer as an infinite sheet of positive charge, and using $r_{41}^{6c6c} = 6.93$ Å^2 calculated by $\mathbf{k}\cdot\mathbf{p}$ perturbation theory[1] for CdTe, we obtain $\alpha_{\mathrm{kp}} = 2.2$ meV Å. The Dresselhaus coefficient reads $\beta = \gamma\langle k_z^2\rangle$. Using $\gamma = 43.9$ eVÅ^3 from $\mathbf{k}\cdot\mathbf{p}$ theory[1] and estimating $\langle k_z^2\rangle$ for a square well, we find $\beta_{\mathrm{kp}} = 4.7$ meV Å. Hence, the above experimental determination of α and β is very well supported by these simple estimates.

We are now in a position to make a direct comparison between the magnitude of SO effects at the individual and at the collective level. We find $\widetilde{\alpha} \sim 6\alpha$ and $\widetilde{\beta} \sim 7\beta$, so that $\mathbf{B}_{\mathrm{SO}}^{\mathrm{coll}}(\mathbf{q}) \simeq 6.5\,\mathbf{B}_{\mathrm{SO}}(\mathbf{q})$. Thus, the interplay of Coulomb and SO interactions produces a striking boost of the Rashba and Dresselhaus effects at the collective level, while preserving the balance between both. This organization and enhancement arises mainly from Coulomb-exchange interaction, which naturally tends to align spins: it gives rise to an additional $\mathbf{k}$-dependent magnetic field[24] that exactly compensates the $\mathbf{k}$-dependence of SO fields, together with enhancing their common component aligned with by $\mathbf{B}_{\mathrm{SO}}(\mathbf{q})$.

In conclusion, using a test-bed spin-polarized 2DEG, we have carried out direct optical measurements of SO fields at the individual and at the collective level. The broad, split line of single-particle excitations reflects the spread of individual SO fields due to their momentum dependence. In strong contrast, the SFW remains a sharp line reflecting the precession of a macroscopic spin in a single collective SO field proportional to the excitation momentum $\mathbf{q}$. Due to many-body effects, this field is drastically enhanced with respect to the one acting on individual electrons. Together with the findings of Ref. 11, these results provide a powerful indication that the observed phenomena are universal to collective spin excitations in conducting systems. This remarkable behavior provides a strong incentive for studying these effects in other helical liquids[31] such as in topological insulators, where SO coupling is very large.[32]

We thank M. Bernard and S. Majrab for technical support and B. Jusserand for fruitful discussion. F.B. is supported by a Fondation CFM-JP Aguilar grant. F.P. acknowledges funding from C'NANO IDF and ANR. C.A.U. is supported by DOE Grant DE-FG02-05ER46213. I.D'A. acknowledges support from EPSRC Grant EP/F016719/1 and I.D'A. and F.P. acknowledge support from Royal Society Grant IJP 2008/R1 JP0870232. The research in Poland was partially supported by the European Union within European Regional Development Fund, through grant Innovative Economy (POIG.01.01.02-00-008/08).

*baboux@insp.upmc.fr

†perez@insp.upmc.fr

[1] R. Winkler, *Spin-Orbit Coupling Effects in Two-Dimensional Electron and Hole Systems* (Springer, Berlin, 2003).

[2] Y. K. Kato, R. C. Myers, A. C. Gossard, and D. D. Awschalom, Nature (London) **427**, 50 (2004).

[3] V. Sih, R. C. Myers, Y. K. Kato, W. H. Lau, A. C. Gossard, and D. D. Awschalom, Nat. Phys. **1**, 31 (2005).

[4] S. D. Ganichev, S. A. Tarasenko, V. V. Bel'kov, P. Olbrich, W. Eder, D. R. Yakovlev, V. Kolkovsky, W. Zaleszczyk, G. Karczewski, T. Wojtowicz, and D. Weiss, Phys. Rev. Lett. **102**, 156602 (2009).

[5] M. D'yakonov and V. Perel', Sov. Phys. Solid State **13**, 3023 (1971).

[6] J. D. Koralek, C. P. Weber, J. Orenstein, B. A. Bernevig, S. Zhang, S. Mack, and D. D. Awschalom, Nature (London) **458**, 610 (2009).

[7] M. Studer, G. Salis, K. Ensslin, D. C. Driscoll, and A. C. Gossard, Phys. Rev. Lett. **103**, 027201 (2009).

[8] A. Balocchi, Q. H. Duong, P. Renucci, B. L. Liu, C. Fontaine, T. Amand, D. Lagarde, and X. Marie, Phys. Rev. Lett. **107**, 136604 (2011).

[9] Y. V. Pershin, Phys. Rev. B **75**, 165320 (2007).

[10]S. Kuhlen, K. Schmalbuch, M. Hagedorn, P. Schlammes, M. Patt, M. Lepsa, G. Güntherodt, and B. Beschoten, Phys. Rev. Lett. **109**, 146603 (2012).

[11]F. Baboux, F. Perez, C. A. Ullrich, I. D'Amico, J. Gómez, and M. Bernard, Phys. Rev. Lett. **109**, 166401 (2012).

[12]V. Kalevich and V. Korenov, JETP Lett. **52**, 230 (1990).

[13]L. Meier, G. Salis, I. Shorubalko, E. Gini, S. Schon, and K. Ensslin, Nat. Phys. **3**, 650 (2007).

[14]B. Jussereand, F. Perez, D. R. Richards, G. Karczewski, T. Wojtowicz, C. Testelin, D. Wolverson, and J. J. Davies, Phys. Rev. Lett. **91**, 086802 (2003).

[15]F. Perez, C. Aku-leh, D. Richards, B. Jusserand, L. C. Smith, D. Wolverson, and G. Karczewski, Phys. Rev. Lett. **99**, 026403 (2007).

[16]C. Aku-Leh, F. Perez, B. Jusserand, D. Richards, and G. Karczewski, Phys. Rev. B **83**, 035323 (2011).

[17]A. Pinczuk, S. Schmitt-Rink, G. Danan, J. P. Valladares, L. N. Pfeiffer, and K. W. West, Phys. Rev. Lett. **63**, 1633 (1989).

[18]Also called Stoner excitations in magnetic metals.

[19]J. Gaj, R. Planel, and G. Fishman, Solid State Commun. **29**, 435 (1979).

[20]F. Perez, Phys. Rev. B **79**, 045306 (2009).

[21]C. Rice, D. Wolverson, A. Moskalenko, S. J. Bending, G. Karczewski, and T. Wojtowicz, Phys. Status Solidi c **9**, 1783 (2012).

[22]Y. Bychkov and E. I. Rashba, J. Phys. C **17**, 6039 (1984).

[23]G. Dresselhaus, Phys. Rev. **100**, 580 (1955).

[24]C. A. Ullrich and M. E. Flatté, Phys. Rev. B **68**, 235310 (2003).

[25]S. M. Badalyan, A. Matos-Abiague, G. Vignale, and J. Fabian, Phys. Rev. B **79**, 205305 (2009).

[26]B. Jusserand, D. Richards, H. Peric, and B. Etienne, Phys. Rev. Lett. **69**, 848 (1992).

[27]This splitting has to be distinguished from the splitting due to the change of kinetic energy between the initial and final electronic states. This quantity, of order $\hbar v_F q$ (with v_F the Fermi velocity), is relevant at bigger q as shown in Ref. 16. Here, in Fig. 4, $\hbar v_F q \simeq 0.06$ meV is very small in comparison to the SO-induced splitting.

[28]G. Giuliani and G. Vignale, *Quantum Theory of the Electron Liquid* (Cambridge University Press, Cambridge, 2005).

[29]Since q is negligible in comparison to the Fermi momentum $k_F \sim 150\ \mu\text{m}^{-1}$ and $Z^* \gg \alpha k_F$ and βk_F, the change of spin orientation between the initial and final electronic states can be neglected.

[30]J. Gómez, F. Perez, E. M. Hankiewicz, B. Jusserand, G. Karczewski, and T. Wojtowicz, Phys. Rev. B **81**, 100403(R) (2010).

[31]S. Raghu, S. B. Chung, X.-L. Qi, and S.-C. Zhang, Phys. Rev. Lett. **104**, 116401 (2010).

[32]P. D. C. King, R. C. Hatch, M. Bianchi, R. Ovsyannikov, C. Lupulescu, G. Landolt, B. Slomski, J. H. Dil, D. Guan, J. L. Mi, E. D. L. Rienks, J. Fink, A. Lindblad, S. Svensson, S. Bao, G. Balakrishnan, B. B. Iversen, J. Osterwalder, W. Eberhardt, F. Baumberger, and P. Hofmann, Phys. Rev. Lett. **107**, 096802 (2011).